

BTZO-1, a Cardioprotective Agent, Reveals that Macrophage Migration Inhibitory Factor Regulates ARE-Mediated Gene Expression

Haruhide Kimura,^{1,*} Yoshimi Sato,¹ Yasukazu Tajima,¹ Hirobumi Suzuki,¹ Hiroshi Yukitake,¹ Toshihiro Imaeda,¹ Masahiro Kajino,¹ Hideyuki Oki,¹ Masayuki Takizawa,¹ and Seiichi Tanida¹

¹Pharmaceutical Research Division, Takeda Pharmaceutical Co. Ltd., 17-85, Jusohonmachi 2-chome, Yodogawa-ku, Osaka 532-8686, Japan

*Correspondence: kimura_haruhide@takeda.co.jp

DOI 10.1016/j.chembiol.2010.10.011

SUMMARY

In a screening program to discover therapeutic drugs for heart diseases, we identified BTZO-1, a 1,3-benzothiazin-4-one derivative, which activated antioxidant response element (ARE)-mediated gene expression and suppressed oxidative stress-induced cardiomyocyte apoptosis in vitro. An active BTZO-1 derivative for ARE-activation protected heart tissue during ischemia/reperfusion injury in rats. Macrophage migration inhibitory factor (MIF), which is known to protect cells from oxidative insult, was identified as a specific BTZO-1-binding protein. BTZO-1 binds to MIF with a K_d of 68.6 nM, and its binding required the intact N-terminal Pro1. MIF, in the presence of BTZO-1, activated the glutathione S-transferase Ya subunit (GST Ya) gene ARE, whereas reduction of cellular MIF protein levels by siRNA suppressed BTZO-1-induced GST Ya expression. These results suggest that BTZO-1 activates the GST Ya gene ARE by interacting with MIF.

INTRODUCTION

Heart disease, including heart failure and myocardial infarction (MI), is associated with high mortality in modern Western societies (Cleland et al., 2001). A key predictor for the development of heart failure is the presence of left ventricular hypertrophy, and the progressive deterioration of the hypertrophied left ventricle (LV) may be related to progressive loss of cardiomyocytes, at least in part, via apoptosis (van Empel et al., 2005). Apoptosis has also been detected in heart tissue at all stages of MI (Abbate et al., 2006). Thus, apoptosis may be responsible for a significant amount of cardiomyocyte death during the acute ischemic stage, as well as for the progressive loss of surviving cells during the subacute and chronic stages. Cardiomyocytes are terminally differentiated and lose their proliferative capacity (Akazawa and Komuro, 2003). Therefore, loss of cardiomyocytes results in a permanent reduction in the number of functioning units in the myocardium. Inhibitors of cardiomyocyte apoptosis could be novel therapeutic agents for cardiovascular diseases.

Here, we describe the identification of 2-pyridin-2-yl-4H-1,3-benzothiazin-4-one (BTZO-1), which suppressed cardiomyocyte apoptosis in vitro probably via activation of antioxidant response element (ARE)-mediated gene expression. ARE is a *cis*-acting DNA regulatory element involved in the induction of multiple cytoprotective factors, including glutathione S-transferases (GSTs), heme oxygenase-1 (HO-1), and γ -glutamylcysteine synthetase (γ -GCS) (Nguyen et al., 2003b; Chen and Kunsch, 2004; Kaspar et al., 2009), and its activation is considered a mechanism of critical importance for cellular protection against oxidative stress in mammalian cells (Chen and Kunsch, 2004; De Vries et al., 2008). BTZO-2, an active BTZO-1 derivative with a better ADME profile, protected heart tissue during ischemia/reperfusion injury in rats. BTZO-1 appears to be a promising lead compound for the discovery of therapeutics for heart diseases.

We also report the identification of macrophage migration inhibitory factor (MIF), a ubiquitous protein, as a specific BTZO-1-binding protein. MIF has been reported to be released by ischemic heart tissue and to activate the cardioprotective AMP-activated protein kinase (AMPK) pathway (Miller et al., 2008). Several studies have suggested that MIF is a critical upstream regulator of the innate and acquired immune response (Calandra and Roger, 2003). In addition, MIF has been found to have a variety of biological functions such as the regulation of cytokine secretion, counter-regulation of glucocorticoids in inflammation, inhibition of oxidative stress-induced cell death, and activation of components of the mitogen-activated protein kinase and Jun-activation domain-binding protein-1 (Jab-1) pathway; however, its precise function in the majority of cells is not known (Calandra and Roger, 2003; Lolis and Bucala, 2003; Bach et al., 2008). Our results suggest that BTZO-1 activates the rat glutathione S-transferase Ya subunit (GST Ya) gene ARE via binding to MIF.

RESULTS

Identification of BTZO-1

To discover novel therapeutic drugs for heart diseases, we established an in vitro screening assay for inhibitors of cardiomyocyte apoptosis using human leukemia inhibitory factor (hLIF) as a control (Fujio et al., 1997; Sheng et al., 1997). Cell death was induced in the primary culture of neonatal rat cardiomyocytes by serum deprivation for 4 days and then cell viability was assessed using 2-(2-methoxy-4-nitrophenyl)-3-(4-nitrophenyl)-5-(2,4-disulfophenyl)-2H-tetrazolium monosodium salt, WST-8,

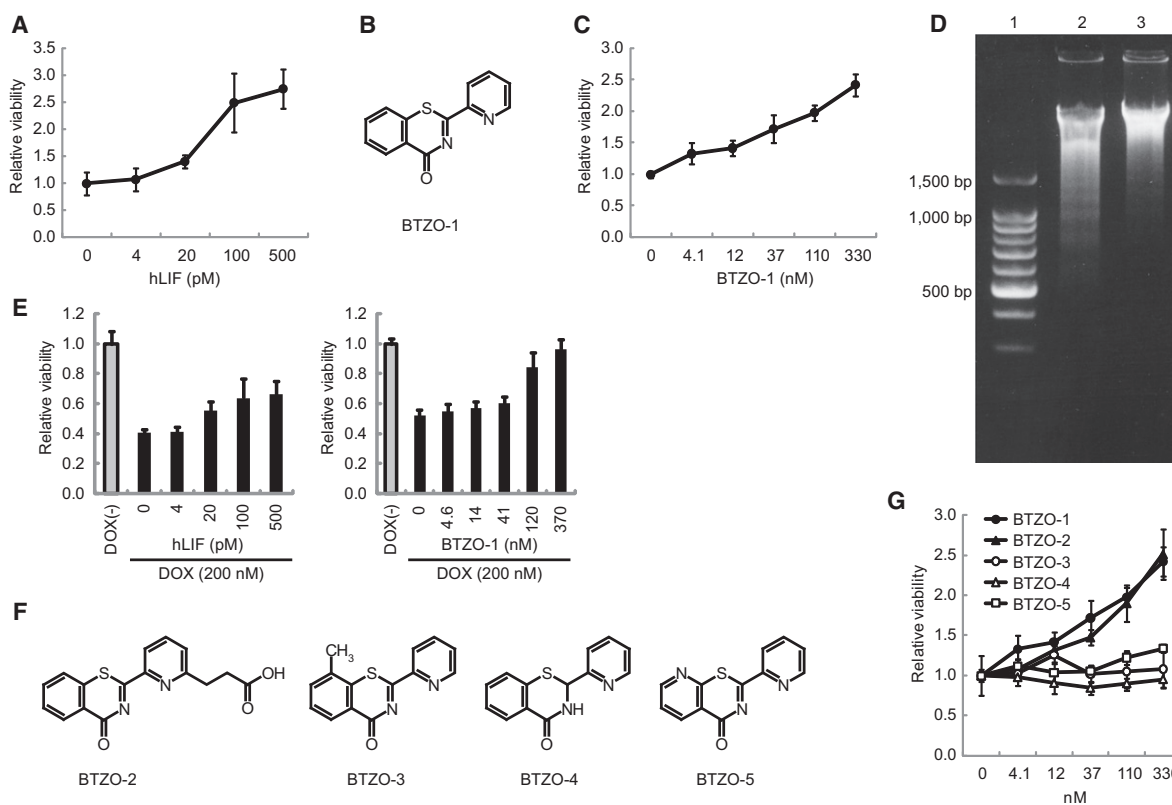


Figure 1. BTZO-1 Suppresses Serum Deprivation or DOX-Induced Cell Death in the Primary Culture of Neonatal Rat Cardiomyocytes

(A) Inhibitory activity of hLIF against serum deprivation-induced cell death in cultured neonatal rat cardiomyocytes. Cell death was induced in cardiomyocytes by culturing in serum-deprived medium for 4 days. Cell viability was determined by the WST-8 assay. Results shown are mean \pm SD, $n = 8$.

(B) Chemical structure of BTZO-1.

(C) Inhibitory activity of BTZO-1 against serum deprivation-induced cardiomyocyte death. Results shown are mean \pm SD, $n = 3$.

(D) Suppression of serum deprivation-induced internucleosomal cleavage of genomic DNA in cardiomyocytes by BTZO-1. Cardiomyocytes were maintained in the presence or absence of $0.37 \mu\text{M}$ BTZO-1 in serum-free media for 3 days and then genomic DNA was isolated and analyzed by electrophoresis on agarose gel. Lane 1 shows the molecular weight marker; lane 2 the control; and lane 3, $0.37 \mu\text{M}$ of BTZO-1.

(E) Inhibitory activity of hLIF or BTZO-1 against DOX-induced death of cardiomyocytes. Cardiomyocytes were pretreated with samples for 3 hr in serum-free medium and then cell death was induced by treatment with 200 nM of DOX for 18 hr. Cell viability was evaluated by the WST-8 assay. Results shown are mean \pm SD, $n = 6$.

(F) Chemical structure of BTZO-1 derivatives.

(G) Inhibitory activity of BTZO-1 derivatives against serum deprivation-induced cardiomyocyte death. Results shown are mean \pm SD, $n = 3$. See also Figure S1.

(WST-8 assay). The hLIF dose dependently increased the number of live cells (Figure 1A). Using this assay, BTZO-1 (Figure 1B) was identified from our chemical library. BTZO-1 dose dependently suppressed serum deprivation-induced cardiomyocyte death; the minimum effective concentration ($\text{MEC}_{1.5}$), defined as the concentration of a sample necessary to give a 50% increase in cell viability, was 16 nM (Figure 1C).

To confirm that the observed cell deaths were secondary to apoptosis, we evaluated cells for the presence of internucleosomal cleavage by monitoring for DNA laddering, a hallmark of apoptosis, on agarose gels (Sheng et al., 1997). Cardiomyocytes caused internucleosomal cleavage of the genomic DNA after culturing for 3 days in serum-free medium, and BTZO-1 at $0.37 \mu\text{M}$ suppressed this internucleosomal cleavage (Figure 1D). These results suggest that the observed cell death is, at least in part, secondary to apoptosis and that BTZO-1 suppressed cardiomyocyte apoptosis. BTZO-1, as well as LIF, also suppressed

doxorubicin (DOX)-induced cell death in cardiomyocytes (Wang et al., 1998) (Figure 1E).

Serum deprivation or stimulation with DOX has been reported to cause oxidative stress; therefore, we suspected that BTZO-1 is an antioxidant. However, BTZO-1 antioxidant activity, measured by 1,1-diphenyl-2-picrylhydrazyl (DPPH) radical scavenging activity, was at least 100 times lower than that of trolox, a vitamin E derivative with potent antioxidant properties (Mickle and Weisel, 1993; Abe et al., 1998). On the other hand, cardiomyocyte apoptosis inhibitory activity of BTZO-1 was about 10,000 times more potent than trolox; the $\text{MEC}_{1.5}$ of trolox was $160 \mu\text{M}$ (see Figures S1A and S1B available online). Thus, BTZO-1 appeared to have a mode of action different from being an antioxidant.

Examination of the structure-activity relationships for BTZO-1 derivatives revealed that introduction of a methyl group at the eight position (BTZO-3), reduction of the C = N bond (BTZO-4),

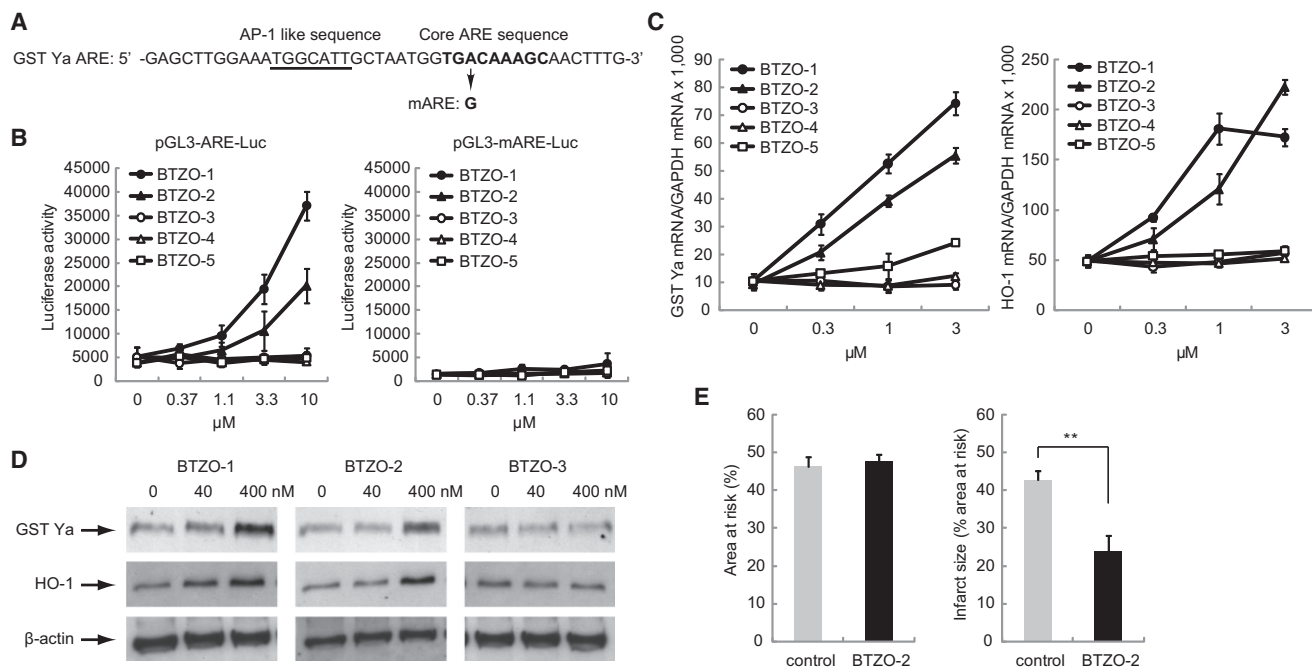


Figure 2. BTZO-1 Activates ARE and Protects Heart Tissue from Ischemia-Reperfusion Injury

(A) Nucleotide sequence of rat GST Ya gene ARE. The core ARE sequence is indicated by the nucleotides in boldface type.

(B) Reporter gene assays showing the effects of BTZO-1 derivatives on ARE activity. H9c2 cells transiently transfected with either pGL3-ARE-Luc or pGL3-mARE-Luc reporter plasmids were treated with BTZO-1 derivatives for 24 hr. Results shown are mean \pm SD, $n = 4$.

(C) BTZO-1 upregulates mRNA levels of GST Ya and HO-1 in cardiomyocytes. Cells were treated with the indicated concentrations of BTZO-1 derivatives for 24 hr in serum-free medium. Messenger RNA levels of GST Ya and HO-1 were measured by real-time quantitative PCR. Results shown are mean \pm SD, $n = 3$.

(D) BTZO-1 upregulates protein levels of GST Ya and HO-1 in cardiomyocytes. Protein extracts were analyzed by western blot analysis with anti-GST Ya (top), anti-HO-1 (middle), or anti- β -actin (bottom) antibodies. β -actin was used as a control.

(E) Effects of BTZO-2 on infarct size following LAD occlusion reperfusion (25 min to 24 hr) in anaesthetized rats. Area at risk is expressed as percentage of the LV. Infarct size is expressed as the percentage of the area at risk. Treatment with BTZO-2 (10 mg/kg, i.p.) 1 hr prior to LAD occlusion, and 2 and 8 hr after reperfusion, significantly reduced the infarct size. Results shown are mean \pm SEM; control, $n = 13$; BTZO-2, $n = 10$. ** $p < 0.01$ versus control. See also Table S1.

or replacement of the phenyl ring of 1,3-benzothiazin-4-one with a pyridine ring (BTZO-5) resulted in a sharp decrease in apoptosis inhibition activity, whereas introduction of a side chain to the pyridine ring, such as a carboxyethyl group (BTZO-2), retained activity; the $\text{MEC}_{1.5}$ of BTZO-2 was 39 nM, whereas those of BTZO-3, BTZO-4, and BTZO-5 were >1000 nM (Figures 1F and 1G).

BTZO-1 Activates ARE-Mediated Gene Expression

Total RNA was recovered from the primary culture of cardiomyocytes cultured in the presence or absence of $0.37 \mu\text{M}$ of BTZO-1 for 21 hr in a serum-free medium and then the global gene expression pattern was investigated using the Affimetrix GeneChip rat genome U34A array, which contains approximately 7000 known genes. Transcription of 89 known genes was upregulated with more than a 2-fold change, and 17 of these were genes possibly induced via ARE (Table S1). ARE activation is important for cellular protection against oxidative stress (Nguyen et al., 2003b; Chen and Kunsch, 2004); therefore, we hypothesized that BTZO-1 inhibits cardiomyocyte apoptosis via induction of cytoprotective factors through ARE activation.

As support for this hypothesis, the effects of BTZO-1 and its derivatives on the induction of ARE-mediated gene expression were investigated using a luciferase reporter assay in H9c2 cells,

a cell line derived from rat cardiac myoblasts. We constructed a pGL3-ARE-Luc reporter plasmid that expressed luciferase under the control of rat GST Ya ARE (Rushmore et al., 1991; Venugopal and Jaiswal, 1998; Dhakshinamoorthy and Jaiswal, 2000). As a control, we also constructed a pGL3-mARE-Luc reporter plasmid in which a point mutation (A \rightarrow G) was introduced into the core sequence (TGACAAAGC) of rat GST Ya ARE that almost completely abolished its activity (Figure 2A) (Rushmore et al., 1991). When H9c2 cells transfected with pGL3-ARE-Luc, but not pGL3-mARE-Luc, were treated with BTZO-1, luciferase activity was induced in a dose-dependent manner (Figure 2B). Thus, the incremental values of luciferase activity in cells transfected with pGL3-ARE-Luc are ARE dependent. Active BTZO-1 derivatives for apoptosis inhibition (BTZO-1 and BTZO-2) induced luciferase activity in a dose-dependent manner, whereas inactive derivatives (BTZO-3, BTZO-4, and BTZO-5) had little or no effect on pGL3-ARE-Luc transfected H9c2 cells (Figure 2B). The $\text{MEC}_{2.0}$ of BTZO-1, BTZO-2, BTZO-3, BTZO-4, and BTZO-5 for ARE activation, which was determined to be the concentration of a compound necessary to double luciferase activity, was 0.82, 2.3, >10 , >10 , and $>10 \mu\text{M}$, respectively (Table 1).

BTZO-1 derivatives showed similar structure-activity relationships in the induction of ARE-regulated cytoprotective genes,

such as GST Ya and HO-1 in the primary culture of neonatal rat cardiomyocytes. Only active derivatives for apoptosis inhibition remarkably increased both GST Ya and HO-1 mRNA levels (Figure 2C); BTZO-1 and BTZO-2, but not BTZO-3, increased protein levels of GST Ya and HO-1 in cardiomyocytes (Figure 2D). These results suggest that BTZO-1 inhibits cardiomyocyte apoptosis via activation of ARE-mediated gene expression.

BTZO-2 Reduces Infarct Size Caused by Myocardial Ischemia/Reperfusion in Rats

The effect of BTZO-2, a BTZO-1 analog with a better ADME profile, on infarct size following ischemia/reperfusion was investigated by measuring the infarct size 24 hr after reperfusion. The mean values for the area at risk were $46\% \pm 3\%$ (vehicle) and $48\% \pm 2\%$ (BTZO-2), respectively (Figure 2E). In rats that received vehicle, left anterior descending coronary artery (LAD) occlusion and reperfusion resulted in an infarct size of 43% of the area at risk (control). When compared to vehicle, intraperitoneal administration (10 mg/kg) of BTZO-2 1 hr prior to LAD occlusion and 2 and 8 hr after reperfusion gave an approximately 45% reduction in infarct size ($p = 0.0013$) (Figure 2E).

Identification of MIF as a Possible BTZO-1 Target Protein

To clarify the molecular mechanisms involved in ARE activation by BTZO-1, we tried to identify possible target protein(s) for BTZO-1 by drug-affinity chromatography (Kimura et al., 2010). Five BTZO-1 derivatives with a carboxy-ethoxypropyl side chain (BTZO-7, BTZO-8, BTZO-9, BTZO-10, and BTZO-11) were prepared for affinity chromatography. BTZO-7 and BTZO-8 are structurally similar to BTZO-1, whereas BTZO-9, BTZO-10, and BTZO-11 are structurally similar to BTZO-3 (BTZO-6), BTZO-4, and BTZO-5, respectively. BTZO-7 and BTZO-8 had potent ARE activation/apoptosis inhibition activity equivalent to that of BTZO-1. In contrast BTZO-9, BTZO-10, and BTZO-11 up to 10 μM did not activate ARE and up to 1 μM did not suppress cardiomyocyte apoptosis, presumably due to introduction of a methyl group at the eight position, reduction of the C = N bond, or replacement of the phenyl ring of the 1,3-benzothiazin-4-one with a pyridine ring, respectively (Table 1).

Protein extracts of rat heart were applied to the two positive columns (BTZO-7 and BTZO-8 columns) and a negative column (BTZO-9 column). After washing the columns with binding buffer, bound proteins were eluted with 1 M NaCl buffer. By analyzing each fraction by SDS-PAGE followed by silver staining, a common binding protein with a molecular mass of approximately 12.5 kDa (indicated by arrows) was identified from the eluted fractions of the two positive columns, but not from the negative BTZO-9-column (Figure 3A). Amino acid sequence analysis revealed that the 12.5 kDa protein was MIF.

Next, we analyzed the binding of BTZO-1 derivatives to purified recombinant rat MIF (rMIF). rMIF was diluted with binding buffer and then was applied to the two positive columns (BTZO-7 and BTZO-8 columns) and the three negative columns (BTZO-9, BTZO-10, and BTZO-11 columns). After washing the columns with binding buffer, bound protein was eluted with an elution buffer containing 1M NaCl. Analysis of each collected fraction by SDS-PAGE followed by silver staining revealed that rMIF was retained on the positive BTZO-7 and BTZO-8 columns,

but not on the negative BTZO-9, BTZO-10, and BTZO-11 columns (Figure 3B). These results suggest that BTZO-1 derivatives active for ARE activation/apoptosis inhibition directly interact with rMIF.

We used a surface plasmon resonance (SPR) biosensor technique to further identify possible target protein(s) of BTZO-1 (Lopez et al., 2003). In this experiment, aminohexylaminocarbonyl variants of BTZO-1 derivatives (BTZO-12 and BTZO-13) were used. BTZO-12 and BTZO-13 are structurally similar to BTZO-1 and BTZO-3, respectively; BTZO-12 retained ARE-activation activity equivalent to that of BTZO-1, whereas BTZO-13 was less potent due to introduction of a methyl group to the eight position of the 1,3-benzothiazin-4-one (Table 1). BTZO-12 and BTZO-13 were each immobilized with a surface density of 655 resonance units (RU) and 816 RU, respectively, on the activated sensor chip CM5 (BTZO-12-type sensor chip and BTZO-13-type sensor chip). The BTZO-12-type sensor chip, but not the BTZO-13-type sensor chip, gave a strong binding signal when protein extract from rat heart was analyzed (Figure 3C). To analyze the bound proteins on the BTZO-12-type sensor chip, we took advantage of a micro-elution procedure available on BIACORE 3000 instruments fitted with a Surface Prep Unit (SPU) (Lopez et al., 2003). Analysis of the recovered fractions by silver staining showed an intense band of low molecular weight (below 16.5 kDa) together with several faint bands, and this low molecular weight protein was confirmed to be MIF by western blot analysis (Figure 3D). Furthermore, the BTZO-12-type sensor chip, but not the BTZO-13-type sensor chip, displayed a strong, direct interaction with rMIF (Figure 3E). These data are in good agreement with the results of the experiments using drug-coupled columns (Figures 3A and 3B). MIF may be a target protein of BTZO-1.

BTZO-1-hMIF Interaction Requires an Intact N-Terminal Pro1

MIF has been predicted to have at least two distinct functional domains: a tautomerase catalytic domain and a thiol-mediated oxidoreductase catalytic domain. Curiously, MIF tautomerase non-physiological substrates like D-dopachrome by its hydrophobic cavity at the N terminus, and the N-terminal proline (Pro1) is involved in the catalytic function (Bendrat et al., 1997; Lubetsky et al., 1999). The cysteine thiol-mediated oxidoreductase catalytic domain of MIF was reported to have a CXXC motif (Kleemann et al., 1998).

To identify the region of MIF that interacts with BTZO-1, we prepared a purified recombinant human MIF protein (hMIF) and five variant forms: substitution of Pro1 with serine (hMIF-P1S) or glycine (hMIF-P1G) (Bendrat et al., 1997; Lubetsky et al., 1999); substitution of the second cysteine in the CXXC motif with serine (hMIF-C59S) (Kleemann et al., 1998); addition of a 30 amino acid peptide with a 6His-tag to the N terminus (His-hMIF); or an eight amino acid peptide with a 6His-tag to the C terminus (hMIF-His) (Figure 4A). The D-dopachrome tautomerase activity of these MIF proteins was spectrophotometrically determined: mutation or blockage of Pro1 (hMIF-P1S, hMIF-P1G, and His-hMIF) resulted in a substantial reduction in catalytic activity, addition of a peptide to the C terminus (hMIF-His) partially reduced the activity, and substitution of cysteine in the

Table 1. Chemical Structure and Activities of BTZO-1 and Its Derivatives

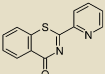
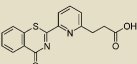
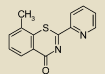
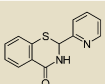
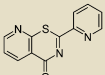
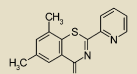
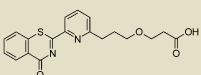
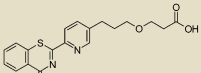
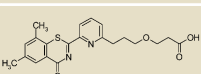
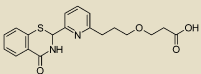
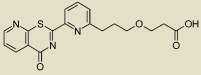
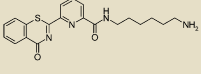
	Chemical Structure	ARE Activation, MEC _{2.0} (μM)	Apoptosis Inhibition, MEC _{1.5} (nM)	Tautomerase Inhibition, % Inhibition at 30 μM
BTZO-1		0.82	16	13
BTZO-2		2.3	39	14
BTZO-3		>10	>1000	6
BTZO-4		>10	>1000	3
BTZO-5		>10	>1000	5
BTZO-6		>10	>1000	ND
BTZO-7		2.2	53	ND
BTZO-8		1.6	39	ND
BTZO-9		>10	>1000	ND
BTZO-10		>10	>1000	ND
BTZO-11		>10	>1000	ND
BTZO-12		1.1	ND	ND

Table 1. Continued

	Chemical Structure	ARE Activation, MEC _{2.0} (μM)	Apoptosis Inhibition, MEC _{1.5} (nM)	Tautomerase Inhibition, % Inhibition at 30 μM
BTZO-13		>10	ND	ND
BTZO-14		0.80	39	12

MEC_{2.0} (μM) for ARE activation was set as the concentration of each compound necessary to double the luciferase activity in pGL3-ARE-Luc reporter plasmid-transfected H9c2 cells. MEC_{1.5} for inhibition of serum deprivation-induced apoptosis was set as the concentration of each sample necessary to give a 50% increase in the viability of cardiomyocytes. Inhibition of rMIF tautomerase activity was measured using L-dopachrome carboxy-methyl ester as a substrate. ND, not determined.

CXXC motif (hMIF-C59S) had little effect on enzymatic activity (Figure 4B; Figure S2A).

The consequence of modulating the interaction with BTZO-1 was evaluated by SPR analysis using the BTZO-12-type sensor chip (BTZO-12 was immobilized with a surface density of 655 RU). N-terminal derivatives (His-hMIF, hMIF-P1S, and hMIF-P1G) resulted in a drastic decrease in interaction, whereas substitution of cysteine in the CXXC motif (hMIF-C59S) or

C-terminal modulation (hMIF-His) had little effect on the interaction (Figure 4C). These data suggest that the intact N-terminal Pro1 is important for BTZO-1 binding, and neither the CXXC motif nor the C terminus is directly involved in the interactions or is necessary for maintaining the active BTZO-1-binding MIF structure.

The effect of BTZO-1 derivatives on rMIF tautomerase activity was assessed using purified L-dopachrome carboxy-methyl ester as a substrate in pH 6.0 buffer. The enzyme reaction

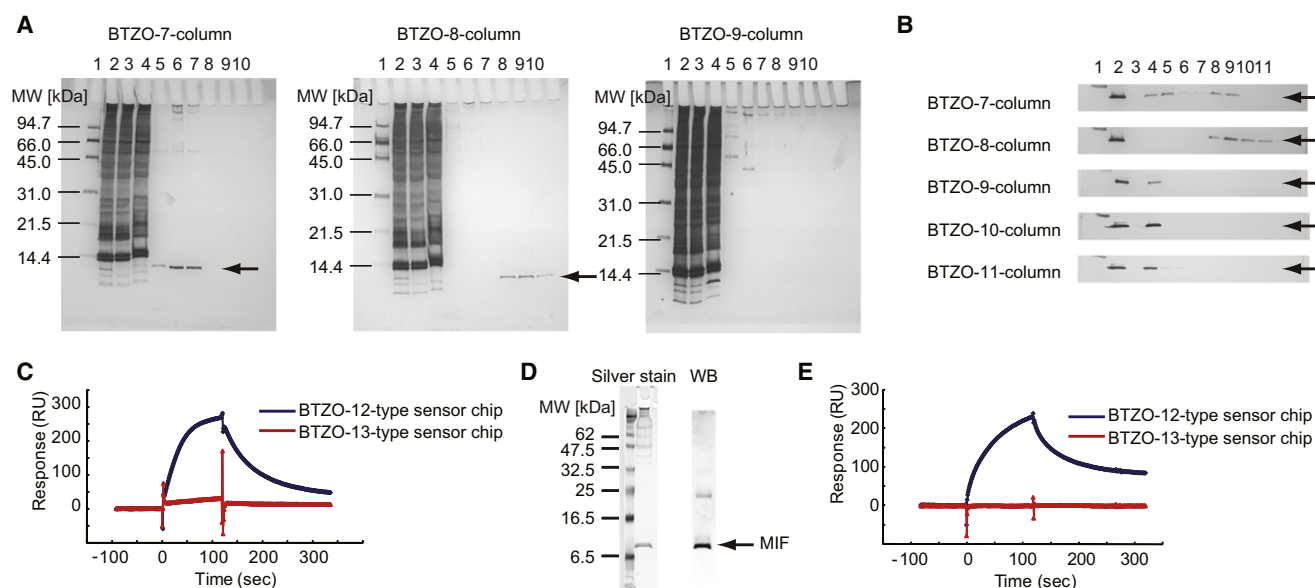


Figure 3. Identification of MIF as a Possible BTZO-1-Binding Protein

(A) Identification of MIF as a possible BTZO-1-binding protein by drug-affinity chromatography. BTZO-7 and BTZO-8 columns were used as positive columns, whereas a BTZO-9 column was used as a negative column. Lane 1 shows molecular weight (MW) marker; lane 2, protein extract from rat heart; lane 3, flow-through fraction; lanes 4 and 5, binding buffer wash fractions; and lanes 6–10, 1 M NaCl-eluted fractions. Arrows indicate the MIF protein.

(B) Direct binding of rMIF to the positive BTZO-7 and BTZO-8 columns. The BTZO-9, BTZO-10, and BTZO-11 columns were used as negative columns. Lane 1 shows the MW marker; lane 2, rMIF; lane 3, flow-through fraction; lanes 4–6, binding buffer wash fractions; and lanes 7–11, 1 M NaCl-eluted fractions. Arrows indicate the rMIF.

(C) Analytical biosensor analysis of rat heart protein extracts using immobilized BTZO-1 derivatives. BTZO-12 was used as a positive compound, and BTZO-13 was used as a negative compound.

(D) Identification of MIF as a major BTZO-12-binding protein. The bound protein was eluted from the BTZO-12-type sensor chip by a microrecovery procedure. Protein identification was achieved by silver staining and western blot (WB) analysis using an anti-MIF antibody.

(E) Direct binding of rMIF to the BTZO-12-type sensor chip. No rMIF binding signal was detected by the BTZO-13-type sensor chip.

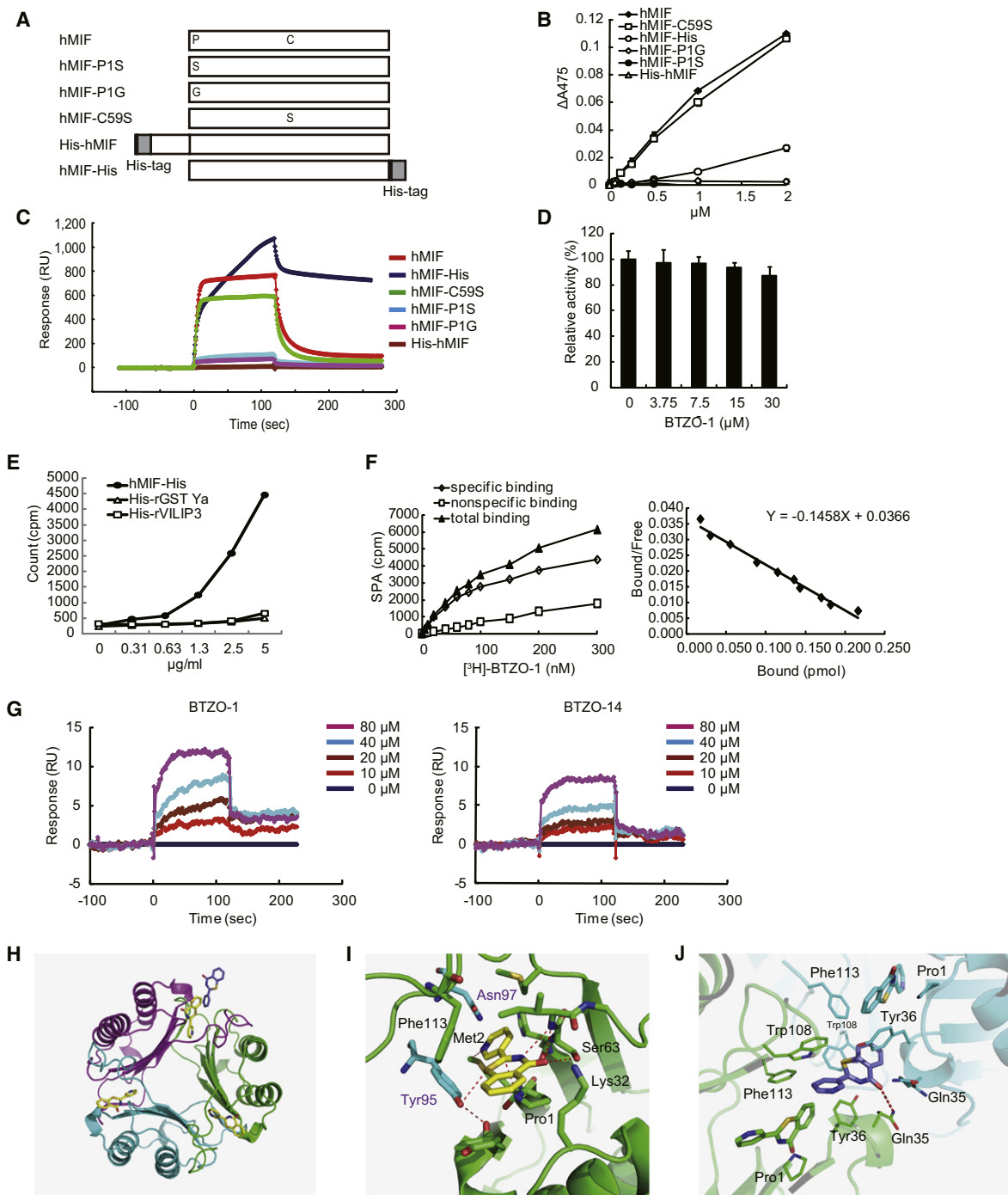


Figure 4. BTZO-1 Binds to MIF with a K_d of 68.6 nM

(A) Schematic representation of hMIF and its mutants (hMIF-P1S, hMIF-P1G, hMIF-C59S, His-hMIF, hMIF-His) employed in the SPR analysis using the BTZO-12-type sensor chip.

(B) Tautomerase activity of hMIF and various mutants using 0.1 mM D-dopachrome as a substrate. Absorbance at 475 nm was measured after 5 min. Results shown are mean \pm SD, $n = 3$.

(C) Evaluation of specific binding of hMIF and various mutants to the BTZO-12-type sensor chip.

(D) Effects of BTZO-1 on the tautomerase activity of rMIF. Purified L-dopachrome carboxy-methyl ester was used as a substrate. Results shown are mean \pm SD, $n = 4$.

(E) SPA measurement of selective [3 H]-BTZO-1 binding to hMIF-His. The 6His-tagged rat GST Ya and rat VILIP3 were used as control proteins. Results shown are mean, $n = 2$.

(F) Analysis of saturation isotherms showing a single saturable high-affinity binding site ($K_d = 68.6$ nM). Results shown are means, $n = 3$.

velocity of rMIF with L-dopachrome carboxy-methyl ester during the initial 30 s was 268 $\mu\text{mol}/\text{min}/\text{mg}$ MIF (Figure S2B). BTZO-1 partially inhibited the tautomerase reaction (Figure 4D and Table 1). Note that the binding affinity of BTZO-1 to rMIF was lower at pH 6.0 than at pH 7.3, as assessed by SPR with BTZO-12 (Figure S2C).

BTZO-1 Interacts with hMIF with a K_d of 68.6 nM

A scintillation proximity assay (SPA) was used to measure the affinity of BTZO-1 to MIF (Kimura et al., 2010). hMIF-His was immobilized on YSi (2–5 μm) copper His-tag SPA beads. Binding of the radioligand [^3H]-BTZO-1 to hMIF-His led to excitation of the scintillant contained in the SPA beads, and the concomitant light emission was measured by beta counter. Specific interactions between hMIF-His and [^3H]-BTZO-1 were detected; however, when other 6His-tagged proteins, such as GST Ya and visinin-like protein 3 (VILIP3), were used instead of hMIF-His, binding of [^3H]-BTZO-1 was not detected, which suggests that BTZO-1 interacts specifically with MIF (Figure 4E). Specific binding was defined as the total binding minus nonspecific binding; nonspecific binding of [^3H]-BTZO-1 to the YSi (2–5 μm) copper His-tag SPA beads was estimated in the absence of hMIF-His. Analysis of the saturation isotherms gave a single saturable high-affinity binding site ($K_d = 68.6$ nM) (Figure 4F). The K_d of BTZO-1 with the 6-His-tagged rat MIF protein (rMIF-His) was 157 nM (Figure S2D). The K_d of BTZO-1 with hMIF, measured by SPR analysis using the BTZO-12-type sensor chip, was 88 nM (Figure S2E).

Crystallography of the hMIF-BTZO-14 Complex

To determine the structural basis for the interaction between BTZO-1 derivatives and MIF, BTZO-14, a BTZO-1 derivative with higher solubility, was co-crystallized with hMIF. BTZO-14 was comparable to BTZO-1 for ARE activation/apoptosis inhibition (Table 1) and for binding affinity to hMIF (Figure 4G). The hMIF-BTZO-14 complex was crystallized as a trimer as previously reported for uncomplexed rat and hMIF (Suzuki et al., 1996; Sun et al., 1996a, 1996b). BTZO-14 bound to the N-terminal Pro1 of each hMIF subunit in the trimer. The carbon atom at the two position of the 1,3-benzothiazin-4-one ring is positioned at a distance of approximately 3.1 \AA from the amino terminus of Pro1, within the sum of the van der Waals radii for carbon and nitrogen atoms (Figures 4H and 4I; Figure S2F). BTZO-14 also bound to the area between the symmetry-related MIF molecules in the crystal structure. This BTZO-14 was positioned between aromatic side chains of Trp108 and Tyr36 from two adjacent MIF molecules and formed a hydrogen bond between the carbonyl oxygen of BTZO-14 and Gln35 (Figures 4H and 4J; Figure S2G).

MIF Induces GST Ya Expression and Suppresses Nitric Oxide-Induced Cardiomyocyte Death

Recent observations that MIF-deficient cells are sensitized to nitric oxide (NO)-induced apoptosis (Mitchell et al., 2002), MIF protects cells from oxidative stress-induced apoptosis (Hudson et al., 1999; Mitchell et al., 2002; Nguyen et al., 2003a), MIF enhances cellular levels of glutathione whose synthesis depends on ARE-regulated γ -GCS (Nguyen et al., 2003a), and MIF induces expression of ARE-regulated GST (Takahashi et al., 2001) suggested a potential regulation of ARE by MIF. Interestingly, MIF could mediate biological activity through either a classical receptor-mediated pathway (Leng et al., 2003; Shi et al., 2006) or a nonclassical endocytic pathway (Calandra and Roger, 2003; Kleemann et al., 2000). Thus, we first evaluated whether rMIF inhibits NO-induced cell death and activates transcription of ARE-regulated genes in cardiomyocytes. Cell death was induced with 30 μM of a NO generator, NOR3, in the presence or absence of rMIF, and then cell viability was measured by the WST-8 assay. rMIF significantly suppressed NO-induced cardiomyocyte death (Figure 5A).

Next, cardiomyocytes were stimulated with rMIF in the presence or absence of 10 μM NOR3 and then the mRNA levels of representative ARE-regulated genes, GST Ya and HO-1, were measured. rMIF stimulation slightly induced GST Ya and HO-1 expression, and NO co-stimulation promoted the rMIF-induced expression of these genes (Figure 5B). rMIF might protect cells from NO-induced death by upregulation of ARE-mediated gene expression. These results, together with the potent and specific binding of BTZO-1 to MIF, prompted us to investigate the molecular mechanisms by which BTZO-1 might induce ARE activation by binding to MIF.

BTZO-1 Promotes MIF-Induced GST Ya ARE Activation

H9c2 cells were stimulated with rMIF in the presence or absence of BTZO-1 and then ARE activation was evaluated by a luciferase reporter assay. BTZO-3, a BTZO-1 derivative with a lower binding affinity to MIF due to introduction of a methyl group to the eight position of the 1,3-benzothiazin-4-one (Figures 3B and 3E, and Table 1), was used as a negative control. Stimulation of pGL3-ARE-Luc transfected H9c2 cells with rMIF in the presence of 1 μM BTZO-1 resulted in a dose-dependent induction of luciferase activity (not observed with pGL3-mARE-Luc transfected cells), whereas stimulation with rMIF and 1 μM BTZO-3 slightly, and with rMIF alone scarcely induced ARE-mediated luciferase activity (Figure 5C). Furthermore, co-stimulation of H9c2 cells with BTZO-1, but not BTZO-3, promoted rMIF induction of GST Ya and HO-1 mRNA (Figure 5D). These results suggest that MIF activates ARE in the presence of some ligand.

Oxygen-free radicals have been implicated in ARE activation; however, BTZO-1 at 10 μM did not cause protein oxidation

(G) Sensorgram showing binding of BTZO-1 or BTZO-14 to immobilized hMIF on a sensor chip CM5 using a SPR biosensor.

(H) The electron density map shows a well-ordered BTZO-14 in complex with the MIF monomer (green); however, in the other MIF monomers (cyan and magenta) of the trimer, the BTZO-14 thiazinone ring is bound in a skewed conformation. BTZO-14 also bound to the area between the symmetry-related MIF molecules (BTZO-14 in purple).

(I) BTZO-14 bound to the vicinity of Pro1 in each MIF monomer. BTZO-14 is shown in yellow, the MIF molecule is highlighted in green, and the neighboring molecule in the trimer is shown in cyan. Hydrogen bonds and other distinct interactions are indicated by red-dashed lines.

(J) BTZO-14 was also positioned between aromatic ring side chains of Trp108 and Tyr36 from both two adjacent MIF molecules. See also Figure S2.

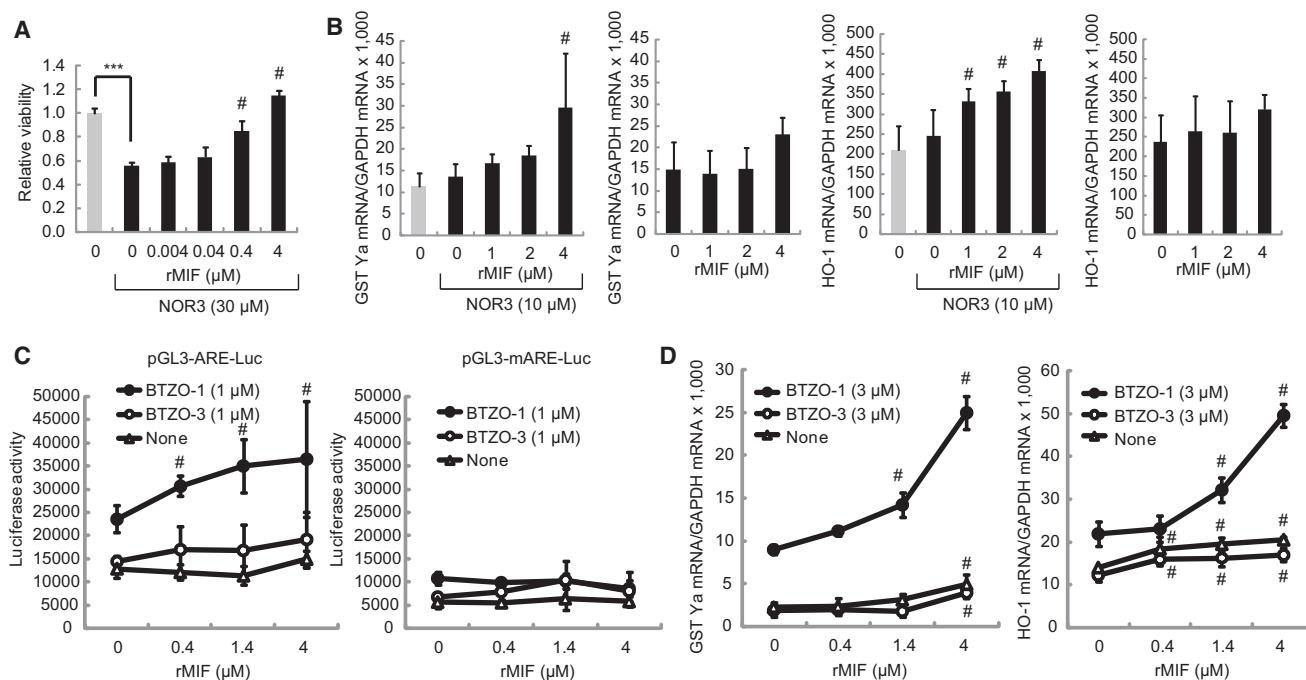


Figure 5. BTZO-1 Promotes rMIF-Induced ARE Activation

(A) rMIF suppresses NO-induced cardiomyocyte death in vitro ($***p \leq 0.001$). Cells were pretreated with the indicated concentrations of rMIF for 3.5 hr and then were treated with 30 μM of NOR3 for 19 hr in serum-free medium. Cell viability was evaluated by the WST-8 assay. Results shown are mean \pm SD, $n = 4$. # $p \leq 0.025$.

(B) rMIF induces GST Ya and HO-1 expression in cardiomyocytes. Cells were stimulated with various concentrations of rMIF in the presence or absence of 10 μM of NOR3 for 3hr (HO-1) or 6hr (GST Ya). Messenger RNA levels of GST Ya and HO-1 were measured by real-time quantitative PCR. Results shown are mean \pm SD, $n = 3$. # $p \leq 0.025$.

(C) BTZO-1, but not BTZO-3, promotes the rMIF-induced ARE activation in H9c2 cells. Cells transiently transfected with either pGL3-ARE-Luc or pGL3-mARE-Luc reporter plasmid were treated with the indicated concentrations of rMIF in the presence or absence of 1 μM BTZO-1 or BTZO-3 for 24 hr. Results shown are mean \pm SD, $n = 4$. # $p \leq 0.025$.

(D) BTZO-1, but not BTZO-3, co-stimulation promoted rMIF-induced GST Ya and HO-1 induction in H9c2 cells. Cells were stimulated with the indicated concentration of rMIF and 3 μM of BTZO-1 derivatives for 6 hr (HO-1) or 24 hr (GST Ya). Messenger RNA levels of GST Ya and HO-1 were measured by real-time quantitative PCR. Results shown are mean \pm SD, $n = 3$. # $p \leq 0.025$. See also Figure S3.

(Figure S3A). To confirm the direct interaction between BTZO-1 and MIF in H9c2 cells, cells were treated with 30 μM of BTZO-1 for 6 hr and then tautomerase activity in the cell lysate was measured. BTZO-1 pretreatment caused an approximately 20% decrease in enzyme activity (Figure S3B), which suggests that there is a direct interaction between BTZO-1 and MIF in H9c2 cells.

Reduction in Cellular MIF Levels Decreases BTZO-1-Induced GST Ya mRNA Expression

We next investigated the effects of reducing the cellular MIF protein level on BTZO-1-induced ARE activation by lowering the MIF mRNA level with small interfering RNA (siRNA). We optimized the conditions for MIF siRNA transfection and cell culture by measuring MIF mRNA levels by real-time PCR analysis and both cellular and medium MIF protein levels by MIF ELISA to attain about 80%, 50%, and 75% reductions of these levels in H9c2 cells, respectively (Figures 6A and 6B). Under these conditions, we could not further transfect pGL3-ARE-Luc; thus, we assessed ARE activation by measuring GST Ya and HO-1 mRNA levels. Induction of GST Ya mRNA expression with 3 μM of

BTZO-1 decreased in the MIF-reduced H9c2 cells, whereas the addition of rMIF to the culture medium restored GST Ya induction (Figures 6C and 6D). HO-1 mRNA showed a similar pattern. These results suggest that BTZO-1 activates ARE-mediated gene expression via binding to MIF.

Interaction of Several Known ARE-Activating Agents and ISO-1 with MIF

The binding of several known ARE-activators, such as *tert*-butylhydroquinone (t-BHQ), Hemin, 15-deoxy-delta-12,14-prostaglandin J2 (15d-PGJ₂), and L-sulforaphane (SFN) (Nguyen et al., 2003b), and ISO-1, a MIF tautomerase inhibitor (Lubetsky et al., 2002), to MIF was measured by [³H]-BTZO-1/rMIF-His SPA, which measured the competitive inhibition of [³H]-BTZO-1 binding to rMIF-His. IC₅₀ values for BTZO-1, t-BHQ, Hemin, 15d-PGJ₂, SFN, and ISO-1 were 0.071, 1.1, 34, 3.6, 25, and >100 μM , respectively. Interestingly, ISO-1 did not activate ARE at concentrations up to 30 μM . Hemin, 15d-PGJ₂, SFN, and ISO-1 also inhibited MIF tautomerase activity (Table S2). Some of the known ARE activators might activate ARE via binding to MIF.

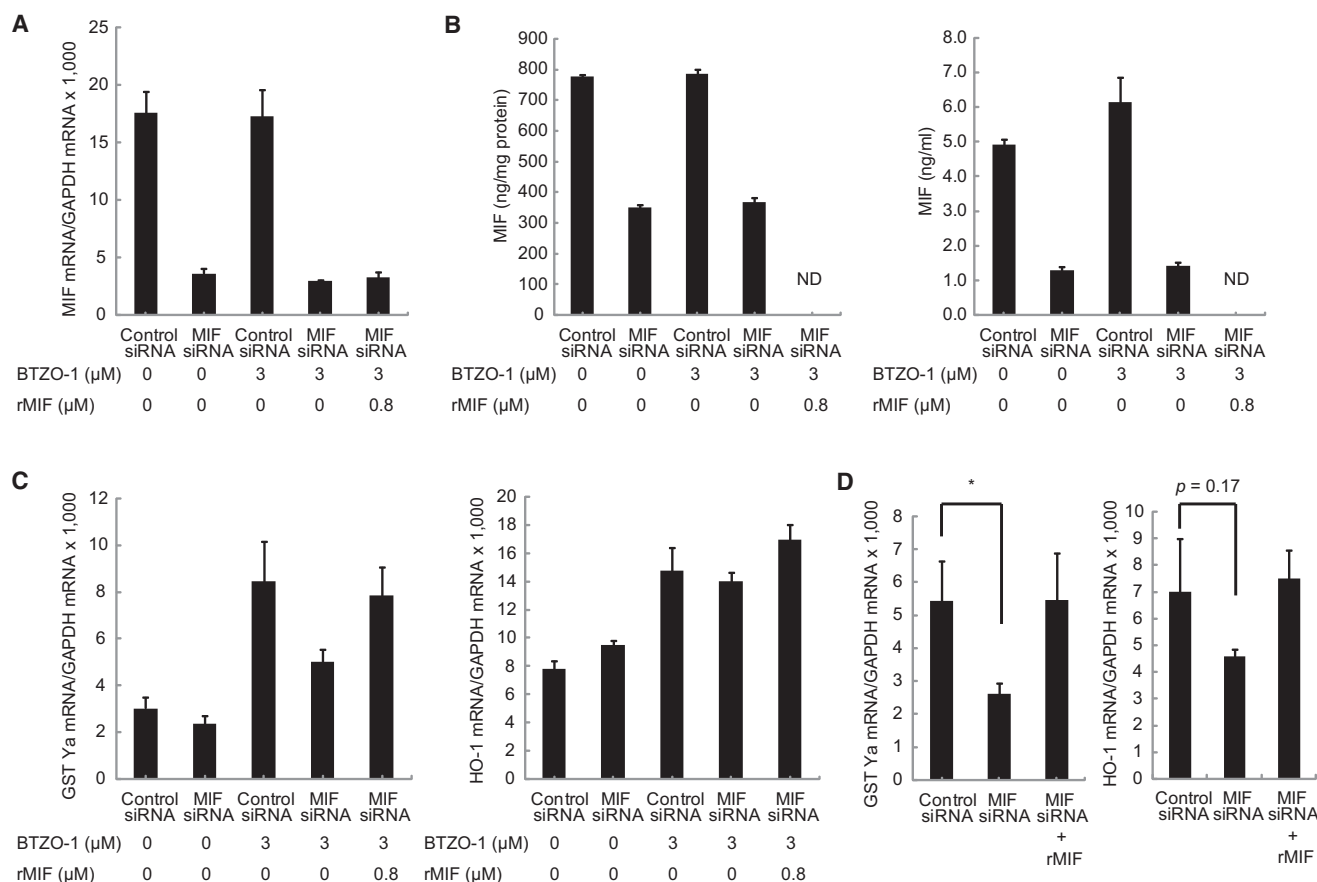


Figure 6. Effects of Reducing the Cellular MIF Protein Level on the BTZO-1-Induced GST Ya and HO-1 Gene Expression in H9c2 Cells

H9c2 cells transfected with control siRNA (control siRNA), or siRNAs directed against rMIF (MIF siRNA) were treated with 3 μM BTZO-1 with or without 0.8 μM rMIF for 24 hr.

(A) Messenger RNA levels of MIF were measured by real-time quantitative PCR. Results shown are mean ± SD, n = 3.

(B) Protein levels of MIF in the cell lysate (left) and culture media (right) were measured by ELISA. Results shown are mean ± SD, n = 3. ND, not determined.

(C) Messenger RNA levels of GST Ya and HO-1 were measured by real-time quantitative PCR. Results shown are mean ± SD, n = 3.

(D) Messenger RNA levels of GST Ya and HO-1 induced by 3 μM of BTZO-1 in H9c2 cells treated with control siRNA, MIF siRNA, or MIF siRNA plus rMIF. Values were obtained from the data shown in (C). Results shown are mean ± SD, n = 3. *p ≤ 0.05. See also Table S2.

DISCUSSION

Cardiomyocyte apoptosis has been hypothesized to be a factor in the initial cause and progression of heart failure. Here, we show that BTZO-1 induced ARE-mediated expression of cytoprotective genes and suppressed cardiomyocyte apoptosis in vitro. BTZO-2, an active BTZO-1 derivative, showed potent cytoprotection against myocardial ischemia/reperfusion injury in rats. Pharmacological activation of endogenous cytoprotective proteins through activation of ARE may serve as a novel strategy for the treatment of heart diseases.

MIF was identified as a target protein for BTZO-1 by drug-affinity chromatography. MIF has been reported to protect cells from oxidative stress-induced cell death (Hudson et al., 1999; Mitchell et al., 2002; Nguyen et al., 2003a). We showed that MIF treatment rescued cardiomyocytes from NO-induced cell death and induced ARE-regulated GST Ya and HO-1 gene expression in vitro. Thus, MIF seemed to be a reasonable target protein for BTZO-1. Further analysis revealed that BTZO-1 deriv-

atives capable of GST Ya ARE activation selectively bound to MIF, BTZO-1 promoted MIF-induced GST Ya ARE activation, and BTZO-1-induced GST Ya induction was suppressed by a reduction in cellular MIF levels. These results suggest that MIF regulates the activation of GST Ya ARE and that BTZO-1, via binding to MIF, acts as an activator of MIF.

ARE activation by MIF seems to require a ligand because NO treatment upregulated MIF-induced GST Ya and HO-1 induction, and BTZO-1, but not BTZO-3, co-stimulation upregulated MIF-induced GST Ya ARE activation and GST Ya and HO-1 mRNA induction. We suspect that NO stimulation caused the production of an unknown internal ligand(s) for MIF. SPR analysis revealed that the BTZO-1-hMIF interaction required the intact N-terminal Pro1. Pro1 and several residues around this site are invariant among all known MIF homologs; Pro1 is nucleophilic due to its location in a hydrophobic environment and has been reported to interact with electrophiles and alkylating agents such as NAPQI (Senter et al., 2002; Lolis and Bucala, 2003). The fact that many ARE-activating agents are electrophiles (Nguyen

et al., 2003b; Chen and Kunsch, 2004) raises the possibility that the MIF N-terminal Pro1 domain functions as a receptor for deleterious electrophiles. Whether other ARE-activating agents function by binding to MIF is worthy of additional investigation.

The binding affinity of ISO-1, which typically binds to a deep pocket near Pro-1 (Lubetsky et al., 2002), to the BTZO-1 binding site in MIF was at least 1000 times less potent than BTZO-1, whereas ISO-1 was more potent than BTZO-1 in inhibiting tautomerase activity. Moreover, ISO-1 was at least 30 times less potent than BTZO-1 in ARE activation. Thus, we speculate that BTZO-1 binds to a different site than ISO-1 in solution. The co-crystallization study with BTZO-14 revealed two possible BTZO-1 binding sites: the canonical MIF inhibitor binding site; and a latent site at the interface area between adjacent symmetry-related MIF molecules, which is nearly identical to the reported cryptic "hydrophobic rim" binding site (McLean et al., 2010) or the allosteric binding site (Cho et al., 2010). Although the space groups and crystal packing of the crystals from the previous studies were different from the crystals in this work, the observed bindings are almost the same. Thus, this latent binding site may not be a crystallization artifact. Moreover, this binding site can account for our enzyme and binding assay results. Further studies are needed to clarify the precise binding site of BTZO-1 in MIF.

The intracellular signaling pathway used by the BTZO-1-MIF complex to activate ARE-mediated gene expression is not yet clear. A decreased cytoplasmic MIF protein level (50%), but not the MIF protein level in the medium (>70%), agrees well with the reduced GST Ya mRNA level induced by 3 μ M of BTZO-1 (50%). Intracellular MIF may mediate the downstream signaling pathway. The addition of 10 μ M of rMIF was needed to restore normal GST Ya mRNA induction caused by 3 μ M of BTZO-1 in MIF-reduced H9c2 cells (50% reduction). Under the conditions used in Figure 2B, MIF levels in the medium and in cells were 3.1 ng/ml and 0.021 pg/cell, respectively, and BTZO-1 stimulation did not affect these MIF levels. If the cell diameter is approximately 10 μ m, the cellular MIF concentrations would reach 1.7 μ M. Thus, it is conceivable that a high concentration of MIF was needed for cellular uptake by endocytosis and to promote MIF-mediated ARE activation. In fact, 3 μ M of MIF was used to induce GST expression in cardiomyocytes (Takahashi et al., 2001).

In conclusion, our results provide new models for both MIF action and ARE activation; binding of BTZO-1 to MIF leads to ARE activation. In inflammatory disease states, high levels of MIF signaling potentially activating additional pathways might be deleterious. However, our study suggests that MIF stimulation by BTZO-1 could protect cells from oxidative insult in some disease states. The discovery of a novel MIF stimulator with such a previously unrecognized mechanism of action was unexpected. Our studies further demonstrate that forward chemical genetics can result in the efficient identification of new drugs and new molecular targets (Kimura et al., 2010).

SIGNIFICANCE

Understanding cellular response to oxidative stress has broad implications for human diseases. In a screening program aimed at discovering therapeutic drugs for heart

diseases, we identified BTZO-1, a 1,3-benzothiazin-4-one derivative, which activated antioxidant response element (ARE)-mediated gene expression and suppressed oxidative stress-induced cardiomyocyte apoptosis in vitro. BTZO-2, an active BTZO-1 derivative for ARE activation, protected heart tissue during ischemia/reperfusion injury in rats. ARE is a cis-acting DNA regulatory element involved in the induction of multiple cytoprotective factors, and its activation is considered a mechanism of critical importance to cellular protection against oxidative stress in mammalian cells. BTZO-1 derivatives might offer a new class of drugs with the potential for treating heart diseases. Macrophage migration inhibitory factor (MIF), which is known to protect cells from oxidative insult, was identified as a specific BTZO-1-binding protein. BTZO-1 bound to MIF with a K_d of 68.6 nM, and its binding required the N-terminal Pro1. MIF, in the presence of BTZO-1, activated the glutathione S-transferase Ya subunit (GST Ya) gene ARE, whereas reduction of cellular MIF protein levels by siRNA suppressed BTZO-1-induced GST Ya expression. MIF has been considered an upstream regulator of innate and acquired immune responses. However, the ubiquitous expression of MIF implies it has biological functions other than immune response. Our results suggest that MIF activates the GST Ya gene ARE in the presence of a ligand, with BTZO-1 the first example of such a MIF ligand.

EXPERIMENTAL PROCEDURES

Isolation of Neonatal Rat Cardiomyocytes

Neonatal rat cardiomyocytes were prepared by proteinase digestion followed by preplating to deplete the cell population of adherent nonmyocardial cells as described previously with some modifications (Fujio et al., 1997).

All animal experiments including isolation of neonatal rat cardiomyocytes were conducted under the guidelines of the Takeda Experimental Animal Care and Use Committee.

Cell Survival Assays

Cell death was induced in cardiomyocytes by serum deprivation at low cell density (3×10^5 cells/ml) for 4 days (Sheng et al., 1997), by DOX treatment (Wang et al., 1998), or by NOR3 treatment. Cell viability was evaluated by the WST-8 assay (Kimura et al., 2010).

ARE-Luc Reporter Assay

The rat GST Ya gene ARE (GAGCTTGAAATGGCATTGCTAATGGTGA CAAAGCAACTTTG) (Dhakshinamoorthy and Jaiswal, 2000) and mutant ARE (GAGCTTGAAATGGCATTGCTAATGGTGGCAAAGCAACTTTG) (Rushmore et al., 1991) were subcloned into the pGL3 vector (Promega) to generate the reporter plasmid pGL3-ARE-Luc and pGL3-mARE-Luc.

H9c2 cells transfected with pGL3-ARE-Luc or pGL3-mARE-Luc were stimulated with BTZO-1 derivatives or 1 μ M of BTZO-1 derivatives together with rMIF for about 24 hr. Cell lysates were prepared using the Steady-Glo Luciferase Assay System (Promega), and luciferase activity was measured with the WALLAC ARVO SX (PerkinElmer, Inc.).

Evaluation of GST Ya and HO-1 Expression

To evaluate the effects of BTZO-1 derivatives on the induction of GST Ya and HO-1 in cardiomyocytes, cells were stimulated with the indicated concentration of various samples or vehicle in Medium 199 (M-199) with 1% penicillin-streptomycin solution (PS) for 24 hr.

To assess the effects of rMIF on GST Ya and HO-1 mRNA levels in cardiomyocytes, cells were cultured with vehicle or the indicated concentration of rMIF in the presence or absence of 10 μ M NOR3 for 3 hr (HO-1) or 6 hr (GST Ya) in M-199 with 1% PS.

When analyzing MIF-induced GSTYa and HO-1 induction in H9c2 cells, cells were stimulated with the indicated concentration of rMIF and 3 μ M of BTZO-1 derivatives in DMEM with 0.5% FBS for 6 hr (HO-1) or 24 hr (GST Ya).

Drug-Affinity Chromatography

BTZO-1 derivatives were coupled to AF-Amino TOYOPEARL (TOSOH Bioscience GmbH) as previously described (Kimura et al., 2010). Binding buffer (10 mM Tris-HCl [pH 7.5], 20% glycerol, 1 mM EDTA, 100 mM NaCl, 0.5 mM p-APMSF, 1 mM DTT) and elution buffer (10 mM Tris-HCl [pH 7.5], 20% glycerol, 1 mM EDTA, 1 M NaCl, 0.5 mM p-APMSF, 1 mM DTT) were used.

SPR Analysis

Interactions of MIF with BTZO-12 or BTZO-13 were examined using the BIACORE 3000 system (GE Healthcare UK Limited) at 25°C. BTZO-12 and BTZO-13 were each immobilized on the activated sensor chip CM5 (BTZO-12-type chip, BTZO-13-type chip). Binding data were analyzed using the BIACORE-3000 control software and the BIA evaluation software (GE Healthcare UK Limited).

SPA

The SPA was set up in 96-well LumiNunc plates (Thermo Fisher Scientific, Inc.) using YSi (2–5 μ m) copper His-tag SPA beads (GE Healthcare UK Limited), [³H]-BTZO-1, and 6His-tagged hMIF or rMIF protein, and a microplate scintillation counter (TopCount NXT; PerkinElmer, Inc.) was used for measurements.

RNA Interference

Small interference RNAs (siRNAs) for rMIF (5'-GCUCAUGACUUUAGUG GC-3') and silencer negative control number 1 siRNA (4611) were obtained from Life Technologies. H9c2 cells were transfected with either MIF siRNA or control siRNA (100 nM) using Opti-MEM (Life Technologies) and Oligofectamine (Life Technologies).

Statistical Analysis

The effect of BTZO-2 on ischemia/reperfusion injury in rats was analyzed by the Aspin-Welch test. In Figure 5, NO-induced cell death (Figure 5A) was analyzed by the t test, GST Ya induction in the presence of NOR3 (Figure 5B), and pGL3-ARE-Luc activation in the presence of BTZO-1 (Figure 5C) were analyzed by the one-tailed Shirley-Williams test, and other experiments were analyzed by the one-tailed Williams's test. In Figure 6D, effects of MIF reduction on drug efficacy were examined by the Aspin-Welch test.

Detailed methods and other procedures are described in the Supplemental Experimental Procedures.

SUPPLEMENTAL INFORMATION

Supplemental Information includes Supplemental Experimental Procedures, three figures, and two tables, and can be found with this article online at doi:10.1016/j.chembiol.2010.10.011.

ACKNOWLEDGMENTS

We wish to express our sincere thanks to Drs. Tadimitsu Kishimoto, Keiko Yamauchi-Takahara, and Hisao Hirota, Osaka University School of Medicine, for their advice on the preparation of the primary culture of cardiomyocytes. We also thank Kaneyoshi Kato, Masaomi Miyamoto, Hideaki Nagaya, Keisuke Hirai, Takenori Ishimaru, Takafumi Ishii, Takashi Horiguchi, Nobuyuki Koyama, Hiroyuki Inuzuka, Takako Fuse, Aki Takiuchi, Akira Kawada, Yutaka Nakayama, Taisuke Tawaraishi, Gyorgy Snell, Shigeru Igaki, Yumiko Moriya, Yumi Hayano, Noriyuki Habuka, Atsushi Nakatani, Hiroaki Omae, and Takashi Ito for their support and/or critical reading of the manuscript.

Received: April 22, 2010

Revised: October 8, 2010

Accepted: October 12, 2010

Published: December 21, 2010

REFERENCES

- Abbate, A., Bussani, R., Amin, M.S., Vetrovec, G.W., and Baldi, A. (2006). Acute myocardial infarction and heart failure: role of apoptosis. *Int. J. Biochem. Cell Biol.* 38, 1834–1840.
- Abe, N., Murata, T., and Hirata, A. (1998). Novel DPPH radical scavengers, bisorbicillinol and demethyltrichodimerol, from a fungus. *Biosci. Biotechnol. Biochem.* 62, 661–666.
- Akazawa, H., and Komuro, I. (2003). Roles of cardiac transcription factors in cardiac hypertrophy. *Circ. Res.* 92, 1079–1088.
- Bach, J.P., Rinn, B., Meyer, B., Dodel, R., and Bacher, M. (2008). Role of MIF in inflammation and tumorigenesis. *Oncology* 75, 127–133.
- Bendrat, K., Al-Abed, Y., Callaway, D.J.E., Peng, T., Calandra, T., Metz, C.N., and Bucala, R. (1997). Biochemical and mutational investigations of the enzymatic activity of macrophage migration inhibitory factor. *Biochemistry* 36, 15356–15362.
- Calandra, T., and Roger, T. (2003). Macrophage migration inhibitory factor: a regulator of innate immunity. *Nat. Rev. Immunol.* 3, 791–800.
- Chen, X.L., and Kunsch, C. (2004). Induction of cytoprotective genes through Nrf2/antioxidant response element pathway: a new therapeutic approach for the treatment of inflammatory diseases. *Curr. Pharm. Des.* 10, 879–891.
- Cho, Y., Crichlow, G.V., Vermeire, J.J., Leng, L., Du, X., Hodsdon, M.E., Bucala, R., Cappello, M., Gross, M., Gaeta, F., et al. (2010). Allosteric inhibition of macrophage migration inhibitory factor revealed by ibudilast. *Proc. Natl. Acad. Sci. USA* 107, 11313–11318.
- Cleland, J.G.F., Khand, A., and Clark, A. (2001). The heart failure epidemic: exactly how big is it? *Eur. Heart J.* 22, 623–626.
- De Vries, H.E., Witte, M., Hondius, D., Rozemuller, A.J.M., Drukarch, B., Hoozemans, J., and Van Horssen, J. (2008). Nrf2-induced antioxidant protection: a promising target to counteract ROS-mediated damage in neurodegenerative disease? *Free Radic. Biol. Med.* 45, 1375–1383.
- Dhakshinamoorthy, S., and Jaiswal, A.K. (2000). Small Maf (MafG and MafK) proteins negatively regulate antioxidant response element-mediated expression and antioxidant induction of the NAD(P)H:Quinone oxidoreductases 1 gene. *J. Biol. Chem.* 275, 40134–40141.
- Fujio, Y., Kunisada, K., Hirota, H., Yamauchi-Takahara, K., and Kishimoto, T. (1997). Signals through gp130 upregulate bcl-x gene expression via STAT1-binding cis-element in cardiac myocytes. *J. Clin. Invest.* 99, 2898–2905.
- Hudson, J.D., Shoabi, M.A., Maestro, R., Carnero, A., Hannon, G.J., and Beach, D.H. (1999). A proinflammatory cytokine inhibits p53 tumor suppressor activity. *J. Exp. Med.* 190, 1375–1382.
- Kaspar, J.W., Niture, S.K., and Jaiswal, A.K. (2009). Nrf2:INrf2 (Keap1) signaling in oxidative stress. *Free Radic. Biol. Med.* 47, 1304–1309.
- Kimura, H., Yukitake, H., Tajima, Y., Suzuki, H., Chikatsu, T., Morimoto, S., Funabashi, Y., Omae, H., Ito, T., Yoneda, Y., and Takizawa, M. (2010). ITZ-1, a client-selective Hsp90 inhibitor, efficiently induces heat shock factor 1 activation. *Chem. Biol.* 17, 18–27.
- Kleemann, R., Kapurniotu, A., Frank, R.W., Gessner, A., Mischke, R., Flieger, O., Jüttner, S., Brunner, H., and Bernhagen, J. (1998). Disulfide analysis reveals a role for macrophage migration inhibitory factor (MIF) as thiol-protein oxidoreductase. *J. Mol. Biol.* 280, 85–102.
- Kleemann, R., Hausser, A., Geiger, G., Mischke, R., Burger-Kentischer, A., Flieger, O., Johannes, F.J., Roger, T., Calandra, T., Kapurniotu, A., et al. (2000). Intracellular action of the cytokine MIF to modulate AP-1 activity and the cell cycle through Jab1. *Nature* 408, 211–216.
- Leng, L., Metz, C.N., Fang, Y., Xu, J., Donnelly, S., Baugh, J., Delohery, T., Chen, Y., Mitchell, R.A., and Bucala, R. (2003). MIF signal transduction initiated by binding to CD74. *J. Exp. Med.* 197, 1467–1476.
- Lolis, E., and Bucala, R. (2003). Macrophage migration inhibitory factor. *Expert Opin. Ther. Targets* 7, 153–164.
- Lopez, F., Pichereaux, C., Bulet-Schiltz, O., Pradayrol, L., Monsarrat, B., and Esteve, J.P. (2003). Improved sensitivity of biomolecular interaction analysis mass spectrometry for the identification of interacting molecules. *Proteomics* 3, 402–412.

- Lubetsky, J.B., Swope, M., Dealwis, C., Blake, P., and Lolis, E. (1999). Pro-1 of macrophage migration inhibitory factor functions as a catalytic base in the phenylpyruvate tautomerase activity. *Biochemistry* 38, 7346–7354.
- Lubetsky, J.B., Dios, A., Han, J., Aljabari, B., Ruzsicska, B., Mitchell, R., Lolis, E., and Al-Abed, Y. (2002). The tautomerase active site of macrophage migration inhibitory factor is a potential target for discovery of novel anti-inflammatory agents. *J. Biol. Chem.* 277, 24976–24982.
- McLean, L.R., Zhang, Y., Li, H., Choi, Y.M., Han, Z., Vaz, R.J., and Li, Y. (2010). Fragment screening of inhibitors for MIF tautomerase reveals a cryptic surface binding site. *Bioorg. Med. Chem. Lett.* 20, 1821–1824.
- Mickle, D.A., and Weisel, R.D. (1993). Future directions of vitamin E and its analogues in minimizing myocardial ischemia-reperfusion injury. *Can. J. Cardiol.* 9, 89–93.
- Miller, E.J., Li, J., Leng, L., MacDonald, C., Atsumi, T., Bucala, R., and Young, L.H. (2008). Macrophage migration inhibitory factor stimulates AMP-activated protein kinase in the ischaemic heart. *Nature* 451, 578–582.
- Mitchell, R.A., Liao, H., Chesney, J., Fingerle-Rowson, G., Baugh, J., David, J., and Bucala, R. (2002). Macrophage migration inhibitory factor (MIF) sustains macrophage proinflammatory function by inhibiting p53: regulatory role in the innate immune response. *Proc. Natl. Acad. Sci. USA* 99, 345–350.
- Nguyen, M.T., Lue, H., Kleemann, R., Thiele, M., Tolle, G., Finkelmeier, D., Wagner, E., Braun, A., and Bernhagen, J. (2003a). The cytokine macrophage migration inhibitory factor reduces pro-oxidative stress induced apoptosis. *J. Immunol.* 170, 3337–3347.
- Nguyen, T., Sherratt, P.J., and Pickett, C.B. (2003b). Regulatory mechanisms controlling gene expression mediated by the antioxidant response element. *Annu. Rev. Pharmacol. Toxicol.* 43, 233–260.
- Rushmore, T.H., Morton, M.R., and Pickett, C.B. (1991). The antioxidant responsive element. *J. Biol. Chem.* 266, 11632–11639.
- Senter, P.D., Al-Abed, Y., Metz, C.N., Benigni, F., Mitchell, R.A., Chesney, J., Han, J., Gartner, C.G., Nelson, S.D., Todaro, G.J., and Bucala, R. (2002). Inhibition of macrophage migration inhibitory factor (MIF) tautomerase and biological activities by acetaminophen metabolites. *Proc. Natl. Acad. Sci. USA* 99, 144–149.
- Sheng, Z., Knowlton, K., Chen, J., Hoshijima, M., Brown, J.H., and Chien, K.R. (1997). Cardiotrophin 1 (CT-1) inhibition of cardiac myocyte apoptosis via a mitogen-activated protein kinase-dependent pathway. *J. Biol. Chem.* 272, 5783–5791.
- Shi, X., Leng, L., Wang, T., Wang, W., Du, X., Li, J., MacDonald, C., Chen, Z., Murphy, J.W., Lolis, E., et al. (2006). CD44 is the signaling component of the macrophage migration inhibitory factor-CD74 receptor complex. *Immunity* 25, 595–606.
- Sun, H.W., Bernhagen, J., Bucala, R., and Lolis, E. (1996a). Crystal structure at 2.6-Å resolution of human macrophage migration inhibitory factor. *Proc. Natl. Acad. Sci. USA* 93, 5191–5196.
- Sun, H.W., Swope, M., Cinquina, C., Bedarkar, S., Bernhagen, J., Bucala, R., and Lolis, E. (1996b). The subunit structure of human macrophage migration inhibitory factor: evidence for a trimer. *Protein Eng.* 9, 631–635.
- Suzuki, M., Sugimoto, H., Nakagawa, A., Tanaka, I., Nishihira, J., and Sakai, M. (1996). Crystal structure of the macrophage migration inhibitory factor from rat liver. *Nat. Struct. Biol.* 3, 259–266.
- Takahashi, M., Nishihira, J., Shimpo, M., Mizue, Y., Ueno, S., Mano, H., Kobayashi, E., Ikeda, U., and Shimada, K. (2001). Macrophage migration inhibitory factor as a redox-sensitive cytokine in cardiac myocytes. *Cardiovasc. Res.* 52, 438–445.
- van Empel, V.P.M., Bertrand, A.T.A., Hofstra, L., Crijns, H.J., Doevendans, P.A., and De Windt, L.J. (2005). Myocyte apoptosis in heart failure. *Cardiovasc. Res.* 67, 21–29.
- Venugopal, R., and Jaiswal, A.K. (1998). Nrf2 and Nrf1 in association with Jun proteins regulate antioxidant response element-mediated expression and coordinated induction of genes encoding detoxifying enzymes. *Oncogene* 17, 3145–3156.
- Wang, L., Ma, W., Markovich, R., Chen, J.W., and Wang, P.H. (1998). Regulation of cardiomyocyte apoptotic signaling by insulin-like growth factor I. *Circ. Res.* 83, 516–522.